



EGF Treatment Improves Motor Behavior and Cortical GABAergic Function in the R6/2 Mouse Model of Huntington's Disease

Felecia M. Marottoli¹ · Mercedes Priego¹ · Eden Flores-Barrera¹ · Rohan Pisharody¹ · Steve Zaldua¹ · Kelly D. Fan¹ · Giri K. Ekkurthi¹ · Scott T. Brady¹ · Gerardo A. Morfini¹ · Kuei Y. Tseng¹ · Leon M. Tai¹

Received: 6 March 2019 / Accepted: 24 April 2019 / Published online: 19 May 2019
© Springer Science+Business Media, LLC, part of Springer Nature 2019

Abstract

Recent evidence indicates that disruption of epidermal growth factor (EGF) signaling by mutant huntingtin (polyQ-htt) may contribute to the onset of behavioral deficits observed in Huntington's disease (HD) through a variety of mechanisms, including cerebrovascular dysfunction. Yet, whether EGF signaling modulates the development of HD pathology and the associated behavioral impairments remain unclear. To gain insight on this issue, we used the R6/2 mouse model of HD to assess the impact of chronic EGF treatment on behavior, and cerebrovascular and cortical neuronal functions. We found that bi-weekly treatment with a low dose of EGF (300 µg/kg, i.p.) for 6 weeks was sufficient to effectively improve motor behavior in R6/2 mice and diminish mortality, compared to vehicle-treated littermates. These beneficial effects of EGF treatment were dissociated from changes in cerebrovascular leakiness, a result that was surprising given that EGF ameliorates this deficit in other neurodegenerative diseases. Rather, the beneficial effect of EGF on R6/2 mice behavior was concomitant with a marked amelioration of cortical GABAergic function. As GABAergic transmission in cortical circuits is disrupted in HD, these novel data suggest a potential mechanistic link between deficits in EGF signaling and GABAergic dysfunction in the progression of HD.

Keywords Epidermal growth factor · GABA · Huntington's disease

Introduction

Huntington's disease (HD) is a neurodegenerative disorder caused by an autosomal dominant genetic mutation that leads

to expansion of a polyglutamine tract (polyQ) in the huntingtin protein (htt) [1, 2]. As a result, progressive motor and cognitive impairments emerge throughout the course of HD [3]. However, the molecular mechanisms contributing to

Felecia M. Marottoli, Mercedes Priego and Eden Flores-Barrera contributed equally to this work.

Electronic supplementary material The online version of this article (<https://doi.org/10.1007/s12035-019-1634-y>) contains supplementary material, which is available to authorized users.

✉ Leon M. Tai
leontai@uic.edu

Felecia M. Marottoli
fmarot2@uic.edu

Mercedes Priego
mpriego@uic.edu

Eden Flores-Barrera
efloresb@uic.edu

Rohan Pisharody
rpisha2@uic.edu

Steve Zaldua
szaldu2@uic.edu

Kelly D. Fan
kfan20@uic.edu

Giri K. Ekkurthi
gekkur2@uic.edu

Scott T. Brady
stbrady@uic.edu

Gerardo A. Morfini
gmorfini@uic.edu

Kuei Y. Tseng
tsengky@uic.edu

¹ Department of Anatomy and Cell Biology, College of Medicine, University of Illinois at Chicago, Chicago, IL 60612, USA

the onset of behavioral abnormalities and associated pathology in HD remain largely unclear. This is in part due to the widespread accumulation of mutant htt (polyQ-htt) in multiple brain regions and cell types [2]. Recent evidence suggests that disruption of growth factor signaling by polyQ-htt [4, 5], including that mediated by epidermal growth factor (EGF) [5–7], could contribute to the onset of behavioral deficits observed in HD. Furthermore, EGF plays a major role in maintaining cerebrovascular function, which is also compromised in HD as revealed by higher cerebrovascular leakiness and altered vessel coverage [8–10]. Mechanistically, disruption of homeostatic mechanisms in the neuronal environment due to cerebrovascular dysfunction could alter glutamatergic and GABAergic function in HD, particularly in the cerebral cortex [8–11]. Alternatively, EGF may also exert direct modulation of glutamatergic [12–15] and GABAergic transmission [16–20]. Through any of these mechanisms, restoring EGF signaling in HD could have beneficial effects on cortical neuronal function and associated behavioral outcomes.

The goal of the present study was to determine whether chronic EGF treatment has beneficial effects in HD through actions on the cerebrovasculature and/or cortical neuronal function. To this end, we employed behavioral, histochemical, and biochemical measures combined with electrophysiology to determine the impact of EGF treatment on motor behavior, cerebrovascular leakiness, and cortical neuronal function in the R6/2 mouse model of HD. This widely used HD model was selected because it expresses a transgene encoding *exon 1* of human polyQ-htt (160 ± 5 glutamines) and exhibits well-characterized HD-relevant behavioral abnormalities and pathology [2, 21].

Methods

Mouse Models and Treatment

All protocols follow the UIC Institutional Animal Care and Use Committee protocols. Mixed male and female R6/2 mice that express the 5' end of the human HD gene containing 160 ± 5 polyQ tracts (JAX002810) were used for this study. EGF (Shenandoah) was reconstituted in sterile water, stored at $-80\text{ }^{\circ}\text{C}$ until the day of treatment. R6/2 or wild-type mice were treated twice a week with $300\text{ }\mu\text{g}/\text{kg}$ EGF or vehicle control (Thursday and Sunday) with an injection volume of $100\text{--}150\text{ }\mu\text{l}$. The dose matches our previous studies in aging and Alzheimer's disease mouse models [22, 23]. Mice for biochemical analysis received a final injection of EGF 30 min prior to sacrifice in order to assess brain and plasma levels after treatment. All investigators were blinded for EGF or vehicle treatment.

Behavioral Testing

The sequence of testing followed the order rotarod (Monday–Wednesday) then open field (Saturday).

Rotarod

Locomotor deficits were evaluated using a modified version of the protocol described in [24]. Mice were first trained once a week for a total of 3 weeks on the rotarod apparatus (San Diego Instruments, CA). During each training session, mice were acclimatized to the apparatus. Acclimatization consisted of placing mice on a rod rotating at a constant speed of 4 rpm for 10 s. The procedure was repeated five times, with a resting interval of approximately 10 s. After this acclimatization procedure was completed, mice were rested for 3 min, then placed on the rod at a constant speed of 4 rpm for 5 min.

For the testing period, mice were tested for three consecutive days. For each training session, mice were first acclimatized to the apparatus as described above and allowed to rest for 20 min. Following acclimatization, three consecutive rotarod trials were performed for each mouse, each separated by 20 min. Rotarod trials consisted of placing mice on an accelerating rod (4–40 rpm). Latency to fall from the rod was recorded for each trial, such that nine measurements were collected over three dates.

Open Field

Open field was used as a measure of locomotor activity/exploratory drive. Open field was conducted in the mouse dark cycle, tracked in real time by an overhead camera, and analyzed using the ANY-Maze software as described in [22, 23]. A single mouse was placed in the center of a white acrylic container ($140\text{ cm} \times w\text{ }30\text{ cm} \times h\text{ }25\text{ cm}$) that contained bedding ($\sim 0.5\text{--}1\text{ in.}$) and allowed to freely explore for 10 min. The distance traveled, average speed ((total distance/total time)-time immobile (defined as periods of immobilization lasting $\geq 5\text{ s}$)) and number of stops (with a stop consisting of 5 s immobilization) were calculated in ANY-Maze.

Biochemical and Immunohistochemical Analysis

Mice were deeply anesthetized with $100\text{ mg}/\text{kg}$ ketamine and $10\text{ mg}/\text{kg}$ xylazine (i.p.), blood drawn by cardiac puncture, and transcardial perfusion performed with PBS as described in [22, 23, 25]. Dissected left hemi-brains were frozen in O.C.T. and stored at $-80\text{ }^{\circ}\text{C}$ until immunohistochemical (IHC) analysis. Right hemi-brains were further dissected into the cortex, which was flash frozen in liquid nitrogen and stored at $-80\text{ }^{\circ}\text{C}$ until processing for biochemical analysis.

Tissue Processing

Cortical samples were weighed and homogenized using a plastic pestle in lysis buffer (1% SDS + 10 mM NaF + 2 mM Na_3VO_4 in HEPES; pH = 7.4) at 5.5 $\mu\text{l}/\text{mg}$ of brain tissue. Homogenates were then incubated in a water bath (90 °C for 2 min), sonicated (20% amplification, 6 cycles), and centrifuged (100,000 $\times g$ for 30 min at 4 °C). Aliquots of the supernatants were flash frozen in liquid nitrogen and stored at –80 °C.

Western Blot Analysis

Levels of neuronal proteins were measured in cortical lysates by western blot total analysis as described in [25]. Protein levels were quantified using the Pierce™ BCA Protein Assay Kit. Twenty micrograms of protein was separated on 26-well, 4–12% Bis-Tris Midi gels (Invitrogen), transferred onto low-fluorescence PVDF membranes, blocked with 5% milk in 0.1% Tween-20 in TBS (TBST), and probed with primary antibodies (list of antibodies and dilutions provided in Supplementary Table 1) in 1% bovine serum albumin in TBS with 0.02% sodium Azide overnight at 4 °C. After washing (3 \times 5 min, TBST), membranes were incubated for 45 min in the appropriate secondary fluorescent secondary antibodies in 1% milk in TBST and 0.01% SDS (LI-COR). Proteins were imaged and quantified using the Odyssey® Fc Imaging System and normalized to either kinesin heavy chain (KHC) or GAPDH. Normalized protein levels were expressed as a ratio of vehicle-treated wild-type mice.

ELISA Analysis

EGF levels were measured in the plasma and cortical brain extracts by ELISA (R&D Systems). Cortical EGF concentrations were normalized to total protein values.

Fibrinogen Extravasation and Laminin Coverage

IHC analysis for fibrinogen extravasation and vessel coverage (laminin) was conducted as described in [22, 23, 25]. Briefly, sagittal sections were taken beginning at the stereotaxic coordinate of ML 3.72 mm through 0 mm in order to encompass the entire cortex. Nine nonadjacent, 12 μm frozen sections (192 μm apart) per animal were fixed with 10% Neutral Buffered Formalin (Sigma). Sections were permeabilized with TBS containing 0.25% triton X-100 (TBSX, 3 \times 5 min), blocked with 5% BSA (2 h), incubated with primary antibodies (4 °C, overnight), washed (3 \times 5 min in TBSX), incubated with secondary antibodies (2 h), washed with TBSX (3 \times 5 min) followed by TBS (1 \times 5 min), and mounted. Fibrinogen (Rabbit anti-fibrinogen 1:200 from Dako, Alexa Fluor 594 anti-rabbit 1:200 from Invitrogen) was co-stained with

CD31 (Rat anti-CD31 from B&D Bioscience with AlexaFluor 488). Laminin was a single stain (rabbit anti-laminin 1:400 from Abcam, AlexaFluor 488 anti-rabbit 1:200 from Invitrogen). Mosaic images were obtained at \times 10 magnification on a Keyence BZ-X microscope with equal exposure settings. The boundaries of each individual brain section were set using the mosaic function, sequential images were obtained encompassing the entire area of the tissue boundary (between ~50 and 150 images per section), and all the individual images were then stitched together to produce a single composite image. Converted images were thresholded equally on ImageJ software (NIH, ImageJ) and quantified using the “Analyze Particles” feature. For representative images, high power magnification (\times 20) images were obtained.

Whole-Cell Patch-Clamp Recordings of Inhibitory Postsynaptic Currents in the Medial Prefrontal Cortex

All experimental procedures including brain slicing and patch-clamp recordings from layer V pyramidal neurons of the medial prefrontal cortex (PFC, infralimbic and prelimbic regions) were conducted as previously described [26, 27]. Briefly, mice were anesthetized with chloral hydrate (400 mg/kg, i.p.) and brains were rapidly removed into ice-cold artificial cerebrospinal fluid (aCSF, 95% O_2 –5% CO_2) to obtain 350- μm -thick PFC slices using a vibrating blade microtome (PELCO, Ted Pella, CA). Slices were then transferred to a holding chamber containing warm aCSF (33–35 °C) constantly oxygenated with 95% O_2 –5% CO_2 for at least 60 min before recording. All recordings were conducted at 33–35 °C using a cesium-based internal solution containing 0.1% Neurobiotin (Vector Laboratories, CA) and (in mM): 140 CsCl, 10 HEPES, 2 MgCl_2 , 5 NaATP, 0.6 NaGTP, and 3 QX-314 (pH 7.23–7.28, 280–282 mOsm). The recording aCSF contained 10 μM of CNQX and 50 μM of APV and (in mM): 122.5 NaCl, 3.5 KCl, 25 NaHCO_3 , 1 NaH_2PO_4 , 2.5 CaCl_2 , 1 MgCl_2 , 20 glucose, and 1 ascorbic acid (pH 7.40–7.43, 295–305 mOsm). GABA_A -mediated inhibitory postsynaptic currents (IPSC) were recorded in voltage-clamp mode at –70 mV. Only neurons exhibiting stable baseline activity (i.e., 10 min) were included for analyses. For comparison, the mean baseline IPSC frequency obtained from at least three noncontiguous epochs of 60 s each was used to determine the effects of the different experimental groups.

Statistical Analysis

All data were analyzed using Chi-squared, one-way ANOVA and Tukey’s post hoc analysis or Student’s *t* test using GraphPad Prism Version 8 as detailed in the figure legend. For electrophysiological studies, the number of cells was used for comparison to better capture the distribution and the extent

of variability across different neurons recorded within a given treatment group.

Results

EGF Improves Motor Behavior in R6/2 Mice

R6/2 mice exhibit pronounced behavioral deficits including locomotor hypoactivity and motor coordination deficits by 10 weeks of age as revealed by impaired performance on rotarod and open-field testing compared to wild-type mice (Supplementary Fig. 1). As reported previously, male and female R6/2 mice exhibited a similar degree of motor behavioral deficits (Supplementary Fig. 1) [28]. Thus, mixed sex cohorts of R6/2 (~30% female mice) and wild-type mice were treated with a bi-weekly low dose of EGF (300 $\mu\text{g}/\text{kg}$, i.p.) or vehicle from 4/5 to 10/11 weeks of age (Supplementary Fig. 2). This dose of EGF was chosen because it does not promote oncogenesis or produce overt signs of toxicity in mice [22, 23, 29].

For all behavioral readouts, we did not observe a significant effect of EGF treatment in wild-type mice (Supplementary Fig. 3). The only exception was a slight decrease in rotarod performance in EGF-treated wild-type mice.

As expected, plasma levels of EGF were higher in both wild-type (Supplementary Fig. 3) and R6/2 mice following EGF treatment (Fig. 1a, left). However, only R6/2 mice showed increased levels of cortical EGF after treatment (Fig. 1a, right), a finding consistent with evidence of a leaky cerebrovasculature in this model. These data suggest that exogenous EGF has increased access to modulate neuronal function in the brain and affect the progression of behavioral deficits in R6/2 mice. Accordingly, the mortality rate of R6/2 mice receiving vehicle treatment was higher than that of EGF-treated mice. During the course of this study, 5 out of 14 vehicle-treated R6/2 mice died compared to 1 out of 15 with EGF treatment ($p < 0.05$, Chi-squared test). Seizures were often seen in vehicle-treated R6/2 mice during handling, at the end of the study prior to sacrifice and immediately prior to death, and we observed fewer seizures in EGF-treated R6/2

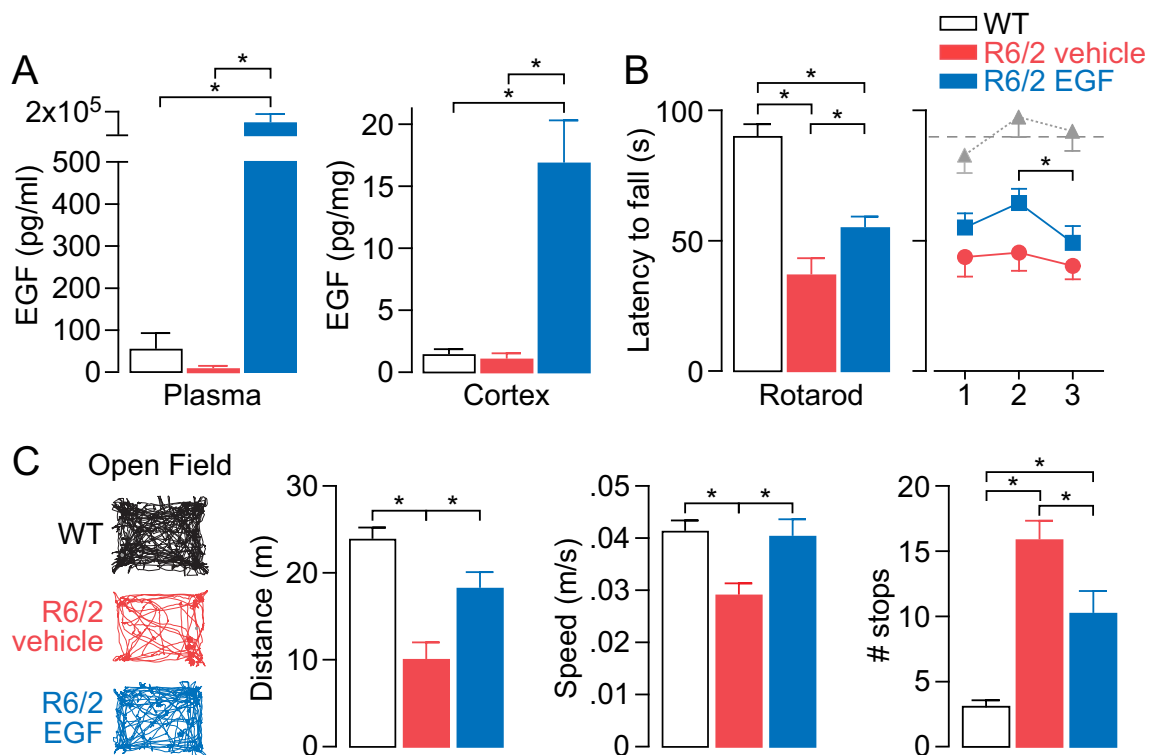


Fig. 1 EGF treatment improves motor behavior in R6/2 mice. Wild-type (WT) or R6/2 mice were treated twice per week with vehicle or EGF (300 $\mu\text{g}/\text{kg}$) from 4/5 to 10/11 weeks of age. **a** Plasma and cortical EGF levels are higher in R6/2 mice after EGF treatment (ELISA). Plasma EGF levels: $F_{(2, 14)} = 24.11$. Brain EGF levels: $F_{(2, 14)} = 24.8$. **b** EGF treatment resulted in improved performance in the rotarod test of motor coordination compared to vehicle treatment in R6/2 mice (left). During the 3 days of rotarod testing, the effect of EGF peaked by day 2 and then declined (right panel). Left, $F_{(2, 21)} = 19$. Right, for EGF-treated R6/2 mice using a repeated measures ANOVA: $F_{(1,912, 21,03)} = 5$. **c** In the

open-field behavioral test, EGF-treated R6/2 mice covered greater distances, moved with a higher average speed, and stopped fewer times compared to vehicle-treated R6/2 mice. Distance: $F_{(2, 25)} = 11.13$. Speed: $F_{(2, 25)} = 5.16$. No. of stops: $F_{(2, 25)} = 10$. Data expressed as mean \pm SEM. * $p < 0.05$ Tukey's post hoc analysis after one-way ANOVA analysis. $n = 5$ per group for WT mice in (a)–(c). In (a), $n = 6$ for vehicle-treated R6/2 mice and 6 for R6/2 EGF-treated mice. In (b), $n = 8$ for vehicle-treated R6/2 mice and 11 for R6/2 EGF-treated mice. In (c), $n = 9$ for vehicle-treated R6/2 mice and 14 for R6/2 EGF-treated mice

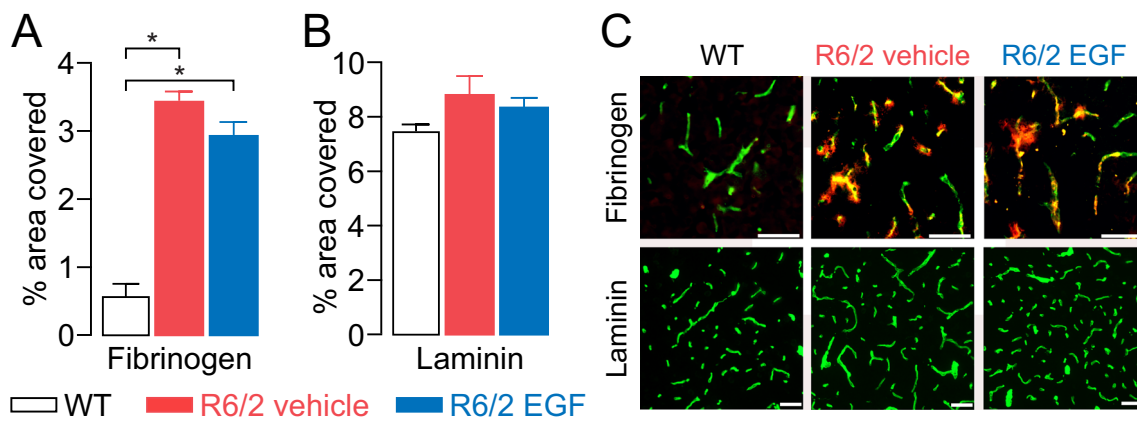


Fig. 2 EGF treatment has no impact on cerebrovascular leakiness or vessel coverage in R6/2 mice. **a** Fibrinogen levels were higher in R6/2 mice compared to wild-type (WT) mice but were unaffected by EGF treatment in the cortex (IHC analysis). $F_{(2, 16)} = 70$. **b** Cortical vessel coverage (laminin staining) was also unaltered by EGF treatment in R6/2 mice. **c** Top, representative images of fibrinogen (red) and brain

endothelial cell (CD31, green) staining in the cortex. Bottom, representative images of laminin (green) staining in cortex. Scale bar, 50 μm. Data expressed as mean ± SEM. * $p < 0.05$ Tukey's post hoc analysis after one-way ANOVA analysis. $n = 5$ for WT mice, 6 for vehicle-treated R6/2 mice, and 8 for EGF-treated R6/2 mice

mice. Since these data were unexpected, our seizure data were observational rather than quantitative. Although life spans were not directly evaluated, these data support that EGF treatment may reduce mortality in R6/2 mice.

In surviving EGF-treated R6/2 mice, motor coordination in the rotarod performance test was significantly improved relative to surviving vehicle-treated R6/2 mice (Fig. 1b). Our standard protocol for rotarod analysis starts 24 h after the last day of treatment and involves three sequential days of testing.

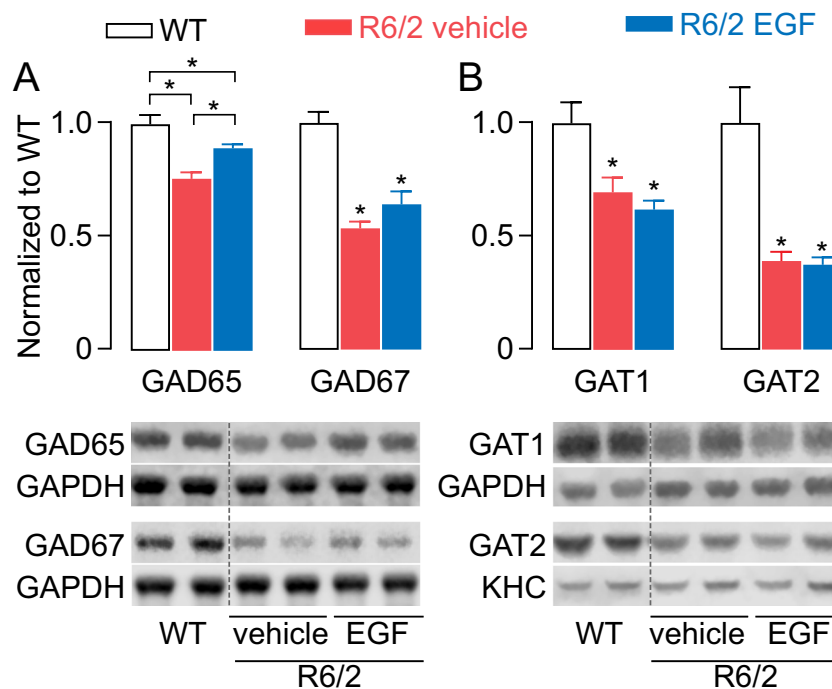


Fig. 3 EGF treatment results in higher GAD65 levels in the cortex of R6/2 mice. When assessed by western blot analysis, compared to vehicle-treated R6/2 mice, EGF treatment resulted in **a** higher GAD65 levels with no changes in GAD67 levels in the cerebral cortex. GAD65 levels: $F_{(2, 14)} = 23$. GAD67 levels: $F_{(2, 14)} = 30$. **b** GAT1 or GAT2 levels were reduced in R6/2 mice compared to wild-type (WT) mice but EGF treatment had no effect. GAT levels: $F_{(2, 14)} = 9.85$. GAT2 levels: $F_{(2, 14)} = 17$. Top, quantification of each protein when normalized to either GAPDH or

KHC as a loading control. All data were then expressed as a ratio to vehicle-treated WT mice. Bottom, representative blots of each protein and loading control, with bands on the same gel in nonadjacent positions separated by a dashed line. Data expressed as mean ± SEM. * $p < 0.05$ Tukey's post hoc analysis compared to vehicle-treated WT mice or the indicated group after one-way ANOVA analysis. $n = 5$ for WT mice, 6 for vehicle-treated R6/2 mice, and 6 for EGF-treated R6/2 mice

When data for all 3 days of testing were pooled, we observed that the latency to fall for EGF-treated R6/2 mice was higher than vehicle-treated R6/2 mice (Fig. 1b, left). Further analysis revealed that the positive impact of EGF treatment on rotarod performance is transient, with a maximal effect at 48 h and followed by a slight decline at 72 h (Fig. 1b, right). EGF treatment also improved the locomotor response of R6/2 mice in the open-field task to wild-type levels when tested within the 24–48-h period following the last EGF treatment (Fig. 1c). Relative to vehicle-treated R6/2 mice, EGF-treated R6/2 mice traveled 80% greater distances with a 40% higher average speed and fewer stops. Collectively, these data demonstrate that chronic bi-weekly EGF treatment can effectively improve locomotor behavior and motor coordination in R6/2 mice.

EGF Does Not Modulate Cerebrovascular Leakiness in R6/2 Mice

The finding that brain EGF levels were higher in R6/2 mice but not wild-type mice after EGF treatment is consistent with higher cerebrovascular leakiness in HD mice. This raised the question of whether a reduction in the extent of cerebrovascular damage after EGF treatment contributed to the improved behavior. To evaluate such a possibility, we assessed cortical levels (extravasation) of the plasma protein fibrinogen, which does not cross into the brain with an intact cerebrovasculature. Relative to wild-type controls, R6/2 mice exhibited higher levels of fibrinogen extravasation. However, EGF treatment of R6/2 mice did not reduce fibrinogen extravasation compared to vehicle treatment (Figs. 2a, c). Similarly, EGF treatment in R6/2 mice failed to alter total vessel coverage, another marker of cerebrovascular dysfunction (Fig. 2b, c). We also found that, while fibrinogen extravasation was higher and vessel coverage lower in the striatum of R6/2 mice compared to wild-type controls, EGF treatment had no effect on either readout in R6/2 mice in the cortex (Supplementary Fig. 4a–c). Collectively, these data indicate that the beneficial effects of EGF are unlikely to result from correcting cerebrovascular defects in R6/2 mice.

Higher GAD65 Levels in the Cortex of EGF-Treated R6/2 Mice

We next explored whether improved neuronal function may contribute to the beneficial effect of EGF treatment on R6/2 mice behavior. Increasing evidence suggests that cortical dysfunction represents an early pathogenic event in HD that contributes to motor deficits. In HD patients, cortical degeneration correlates with behavioral phenotypes [11] and there is cortical degeneration in most HD models analyzed to date, including R6/2 mice [24, 30–32]. Our additional justification was that the balance of excitatory and inhibitory activity is linked

to seizure activity in the cortex, and we anecdotally observed fewer seizures in EGF-treated R6/2 mice. We first assessed cortical levels of an archetypical marker of glutamatergic synapses, PSD95, and found that it was markedly diminished in R6/2 mice relative to wild-type controls (Supplementary Fig. 5). However, EGF treatment did not normalize PSD95 levels in R6/2 mice and similar results were obtained with antibodies for NR1 and NR2A (Supplementary Fig. 5), suggesting that the extent of glutamatergic deficits and the behavioral impact of EGF were not correlated.

Disruption of cortical GABAergic function is also prominent in HD animal models. Indeed, compromised interneuron activity is thought to contribute to cortical hyperexcitability in HD [30–33]. Interestingly, rodent models of disrupted GABAergic activity display a phenotype similar to that seen in R6/2 mice, including seizures and deficits in motor coordination and locomotion [34]. We found that the two isoforms of glutamate decarboxylase (GAD65 and GAD67) that produce GABA were markedly diminished in the cortex (Fig. 3a), but not the striatum (Supplementary Fig. 4) of R6/2 mice, relative to wild-type controls. The lower GAD67 levels in the cortex in R6/2 mice are consistent with previous reports [33, 35]. Interestingly, these two markers of GABAergic function were differentially affected by EGF treatment (Fig. 3a). While GAD65 levels were higher in EGF-treated R6/2 mice compared to vehicle-treated, GAD67 levels remained diminished. We next examined whether other markers of GABAergic function were affected by EGF treatment (Fig. 3b). Relative to wild-type mice, R6/2 mice showed lower levels of the GABA transporters GAT1 and GAT2, a deficit that remained unchanged following EGF treatment. Together, these results suggest that EGF treatment likely involves modulation of selected EGF effectors, rather than overall improvement of interneuron function.

EGF Treatment Normalized Cortical GABAergic Transmission in R6/2 Mice

To determine whether the beneficial effect of EGF treatment in R6/2 mice is associated with an improvement of cortical GABAergic function, we conducted whole-cell patch-clamp recordings in brain slices and compared the extent of GABAergic disruption in the PFC. This brain region was chosen because alterations in PFC neuronal activity have been directly related to the severity of behavioral deficits in R6/2 mice [36] and to locomotor-based behavioral outcomes including open-field and rotarod performances [37–41]. Relative to wild-type controls, the number of spontaneous GABA_AR-mediated IPSC events onto layer V pyramidal neurons was markedly reduced in the PFC of R6/2 mice (Fig. 4a, b). Notably, such GABAergic disruption was not associated with changes in IPSC mean amplitude (wild type, 18.7 ± 2.3 pA; R6/2 vehicle, 19.2 ± 1.5 pA; R6/2 EGF, $19.5 \pm$

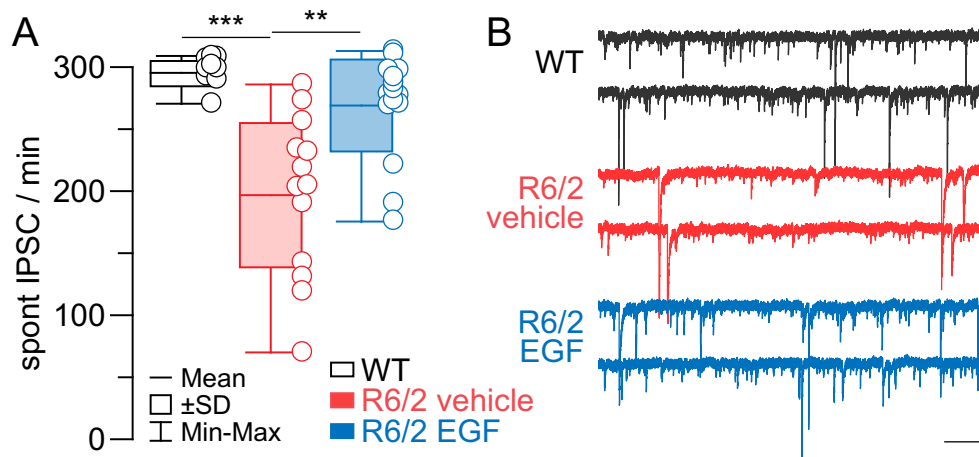


Fig. 4 EGF treatment improves GABAergic transmission in the medial PFC of R6/2 mice. **a** Box plot summarizing the levels of spontaneous (spont) IPSC events recorded from layer V pyramidal neurons in the medial PFC of wild-type (WT) and R6/2 mice. Relative to WT controls ($n = 9$ cells, 3 mice), neurons recorded from vehicle-treated R6/2 mice ($n = 13$ cells, 4 mice) showed a marked reduction in the number of IPSC per min ($***p < 0.0005$, Tukey's post hoc test after significant one-way

ANOVA; $F_{(2, 34)} = 14.18$). Notably, this deficit in IPSC frequency was no longer observed in PFC brain slices obtained from EGF-treated R6/2 mice ($n = 15$ cells, 5 mice; $p = 0.4$ vs. WT mice, $**p < 0.001$ vs. vehicle, Tukey's post hoc test). **b** Traces of spontaneous IPSC recorded from layer V pyramidal neurons in the medial PFC of WT and R6/2 mice (vehicle vs. EGF) illustrating the results shown in (a) (calibration bars, 20 pA/1.5 s)

1.7 pA) or expression levels of GABA_ARs (data not shown). Consistent with the biochemical data (Fig. 3a), EGF treatment effectively increased the frequency of IPSC events to wild-type levels. In sum, these results indicate that the impact of EGF treatment in R6/2 mice could be mediated by normalizing GABAergic transmission in the cerebral cortex.

Discussion

Our data indicate that EGF treatment can diminish mortality and effectively improve locomotor activity and motor coordination in R6/2 mice. Interestingly, the improved rotarod performance peaked at 48 h following the last EGF treatment and then declined at 72 h. These beneficial effects of EGF on motor behavior were not associated with improved cerebrovascular function. Instead, our data indicate that the impact of EGF treatment on R6/2 mice behavior may occur through activation of cortical GABAergic function and/or modulation of polyQ-htt-induced pathogenic events that compromise this function.

Recent studies documented cerebrovascular dysfunction in HD and rodent models of HD including higher permeability [8–10] and increased cerebrovascular density [8, 10, 42]. In agreement with these reports, we found higher fibrinogen extravasation and a trend of higher vessel coverage in the brain of R6/2 mice relative to wild-type controls. Compared to endothelial cells in other organs, brain endothelial cells are highly specialized to limit paracellular diffusion of substances from the peripheral circulation into the brain. Proposed mechanisms by which polyQ-htt induces brain endothelial cell

dysfunction, including intracellular signaling [43] and cell-cell interactions through activated astrocytes [10], are expected to result in higher vascular permeability. Thus, targeting dysfunctional brain endothelial cell pathways in HD (e.g., with EGF) could improve cerebrovascular function and behavioral responses as seen in animal models of other neurodegenerative disorders [22, 23]. However, our study indicates that benefits of EGF treatment did not result from normalization of cerebrovascular function in R6/2 mice. Our results do not preclude the possibility that higher doses or treatment frequency of EGF could overcome brain endothelial cell deficits in HD. The behavioral improvement observed following EGF treatment may result from EGF receptor signaling exerting its action on cortical GABAergic activity.

Increasing evidence suggests that dysfunctional GABAergic transmission plays a major role in the development of behavioral impairments in HD (reviewed in [11, 44]). In support, reduced cortical inhibition in HD correlates with clinical severity when assessed by transcranial magnetic stimulation [45]. A link between GABAergic dysfunction and behavioral impairments has been documented in R6/2 and other HD rodent models [30, 32, 46]. Interestingly, the frequency of spontaneous IPSCs in the cortex of R6/2 mice was reportedly higher at early stages of postnatal development (e.g., P21) and then decreased at a later age (80 days) [46]. Higher IPSCs in younger R6/2 mice is thought to be a compensatory mechanism because inhibiting GABA_A receptors at both P21 and P80 resulted in higher seizures in R6/2 mice [46]. Biochemical analysis further supports functional data on GABAergic dysfunction in HD. For example, there are reports

of lower GABA content in HD patients [47–50] and decreased GABA synthesis in HD mice [33], which are often associated with changes in the subunit composition of GABA receptors (reviewed in [44]). Our biochemical and electrophysiological data are in agreement with these published reports, which reinforce the notion that impaired cortical GABAergic function contributes to the development of behavioral abnormalities in R6/2 mice.

The observation of reduction in seizures and quantification of increased frequency of GABAergic transmission suggests that behavioral effects of EGF treatment in R6/2 mice may occur through improving cortical GABAergic function. Although the expression of EGF receptors in the brain declines during postnatal development, GABAergic cells do express EGF receptors in adult rodents [51]. As a receptor tyrosine kinase, activation of EGF receptors could directly enhance GABAergic function through activation of intracellular signaling cascades, including Ras/ERK/CREB [52] and PKC signaling pathways [53] that are linked to higher GAD65 levels/activity. Thus, one possible mechanism is that EGF receptor activation in GABAergic interneurons increases activity-dependent GABA production as revealed by higher GAD65 levels in R6/2 mice after EGF treatment. Alternatively, EGF treatment may normalize the trafficking and delivery of GAD65 to synapses by promoting specific posttranslational modifications of GAD65 (e.g., palmitoylation) [54] or by counteracting the disrupting effects of polyQ-Htt on axonal transport in HD [55]. In addition, signaling pathways activated by the EGF receptor are also linked to GABA_A receptor sensitivity (reviewed in [56–58]). Based on available data, we propose a mechanism whereby EGF receptor activation on GABAergic interneurons results in higher activity-dependent release of GABA sufficient to restore cortical GABAergic function and motor behavior in R6/2 mice.

Our data provide evidence for targeting cortical EGF system to ameliorate disease progression in HD. However, it remains speculative whether the beneficial effects of EGF are mechanistically linked to the disruptions induced by polyQ-htt. EGF produced a transient effect on performance in the rotarod task. Thus, these data would support a symptomatic benefit. Alternatively, EGF may be targeting mechanistic pathway(s) that are disrupted in HD. Our data support a role of EGF in ameliorating disrupted GABAergic function in the cortex induced by polyQ-htt. Accordingly, EGF treatment may slow disease progression by direct or indirect modulation of signaling pathways disrupted by polyQ-htt. An additional caveat is the rapid disease progression in the R6/2 model, which calls for future validation of the beneficial effects of EGF in a full-length polyQ-htt animal model (i.e., Q175 mice) using different frequencies and doses of treatment.

The neurobiological actions of EGF signaling in R6/2 mice are likely to be complex. PolyQ-htt may negatively impact

GABAergic function and EGF receptor signaling/turnover independently [5–7, 59]. For instance, polyQ-htt is thought to disrupt the function of multiple growth factor receptors, including brain-derived neurotrophic factor ([60] reviewed in [4]) and nerve growth factor [5]. Therefore, EGF treatment may partially compensate for growth factor receptor deficits induced by polyQ-htt in GABAergic neurons. Furthermore, non-neuronal cells such as astrocytes and microglia also express EGF receptors that are disrupted by polyQ-htt in HD [7, 33]. In this regard, the impact of EGF treatment on cortical GABAergic transmission could be a result of ameliorating polyQ-htt-induced metabolic dysfunction in glial cells.

Cortical glutamatergic dysfunction is also a prominent feature in HD and animal models of HD (reviewed in [11]). Accordingly, we observed lower levels of the glutamatergic synaptic marker PSD95 in both the cortex and striatum of R6/2 mice relative to wild-type controls. Although glutamatergic neurons express EGF receptors [12–15], our data indicate that EGF treatment failed to normalize PSD95 levels, but did improve markers of cortical GABAergic activity in R6/2 mice. These results indicate that markers of GABAergic function are more susceptible to EGF treatment in R6/2 mice. Future studies are needed to reveal the cellular and molecular identity of the EGF receptor signaling pathways that enhance cortical GABAergic transmission in R6/2 mice, which in turn could provide novel insights into how a GABAergic dysregulation contributes to HD progression.

Conclusions

In summary, we demonstrated that chronic systemic EGF treatment improves behavioral outcomes in R6/2 mice concurrent with a gain and/or recovery of cortical GABAergic function. These novel data suggest a possible mechanistic link between EGF signaling and the GABAergic system in HD.

Acknowledgments We would like to thank Norma Hernandez for technical assistance with mouse breeding and UL1TR002003, which allowed the use of the Keyence microscope.

Author Contributions L.M.T. and K.Y.T. wrote the manuscript and prepared the figures. L.M.T., F.M.M., G.A.M., S.T.B., and K.Y.T. designed and supervised the study. F.M.M., L.M.T., P.M., R.P., S.Z., K.D.F., G.K.E., and N.H. conducted behavior testing, biochemical, and immunohistochemical analyses. K.Y.T. and E.F. designed and performed the electrophysiological experiments and data analyses. All authors read and approved the final manuscript.

Funding Information Supported by National Institutes of Health Grants (R01AG061114, R21AG053876, and R21AG061715 to L.M.T.; R21NS096642 to G.A.M.), University of Illinois at Chicago institutional start-up funds (L.M.T.), and CHDI research contract No. A-11014 (G.A.M and S.T.B.).

Availability of Data and Materials The datasets used and/or analyzed during the current study are available from the corresponding author on reasonable request.

Compliance with Ethical Standards

Conflict of Interest The authors declare they have no conflict of interest.

Research Involving Human Participants and/or Animals This article does not contain any studies with human participants performed by any of the authors.

Ethical Approval All procedures follow the UIC Institutional Animal Care and Use Committee protocols.

Abbreviations aCSF, Artificial cerebrospinal fluid; EGF, Epidermal growth factor; GAD, Glutamate decarboxylase; HD, Huntington's disease; htt, Huntingtin protein; polyQ-htt, Mutant htt; IHC, Immunohistochemical; IPSC, Inhibitory postsynaptic currents; KHC, Kinesin heavy chain; PFC, Prefrontal cortex; R6/2 mice, Mice that express the 5' end of the human HD gene containing 160 ± 5 poly Q; TBSX, TBS containing 0.25% triton X-100

References

- Gusella JF, Wexler NS, Conneally PM, Naylor SL, Anderson MA, Tanzi RE, Watkins PC, Ottina K et al (1983) A polymorphic DNA marker genetically linked to Huntington's disease. *Nature* 306(5940):234–238
- Han I, You Y, Kordower JH, Brady ST, Morfini GA (2010) Differential vulnerability of neurons in Huntington's disease: the role of cell type-specific features. *J Neurochem* 113(5):1073–1091. <https://doi.org/10.1111/j.1471-4159.2010.06672.x>
- Roze E, Bonnet C, Betuing S, Caboche J (2010) Huntington's disease. *Adv Exp Med Biol* 685:45–63
- Bodai L, Marsh JL (2012) A novel target for Huntington's disease: ERK at the crossroads of signaling. The ERK signaling pathway is implicated in Huntington's disease and its upregulation ameliorates pathology. *Bioessays* 34(2):142–148
- Song C, Perides G, Liu YF (2002) Expression of full-length polyglutamine-expanded huntingtin disrupts growth factor receptor signaling in rat pheochromocytoma (PC12) cells. *J Biol Chem* 277(8):6703–6707. <https://doi.org/10.1074/jbc.M110338200>
- Melone MA, Calarco A, Petillo O, Margarucci S, Colucci-D'Amato L, Galderisi U, Koverech G, Peluso G (2013) Mutant huntingtin regulates EGF receptor fate in non-neuronal cells lacking wild-type protein. *Biochim Biophys Acta* 1832(1):105–113. <https://doi.org/10.1016/j.bbadis.2012.09.001>
- Lievens JC, Rival T, Iche M, Chneiweiss H, Birman S (2005) Expanded polyglutamine peptides disrupt EGF receptor signaling and glutamate transporter expression in *Drosophila*. *Hum Mol Genet* 14(5):713–724. <https://doi.org/10.1093/hmg/ddi067>
- Lin CY, Hsu YH, Lin MH, Yang TH, Chen HM, Chen YC, Hsiao HY, Chen CC et al (2013) Neurovascular abnormalities in humans and mice with Huntington's disease. *Exp Neurol* 250:20–30. <https://doi.org/10.1016/j.expneurol.2013.08.019>
- Di Pardo A, Amico E, Scalabri F, Pepe G, Castaldo S, Elifani F, Capocci L, De Sanctis C et al (2017) Impairment of blood-brain barrier is an early event in R6/2 mouse model of Huntington disease. *Sci Rep* 7:41316. <https://doi.org/10.1038/srep41316>
- Hsiao HY, Chen YC, Huang CH, Chen CC, Hsu YH, Chen HM, Chiu FL, Kuo HC et al (2015) Aberrant astrocytes impair vascular reactivity in Huntington disease. *Ann Neurol* 78(2):178–192. <https://doi.org/10.1002/ana.24428>
- Estrada-Sanchez AM, Rebec GV (2013) Role of cerebral cortex in the neuropathology of Huntington's disease. *Front Neural Circuits* 7:19. <https://doi.org/10.3389/fncir.2013.00019>
- Tang Y, Ye M, Du Y, Qiu X, Lv X, Yang W, Luo J (2015) EGFR signaling upregulates surface expression of the GluN2B-containing NMDA receptor and contributes to long-term potentiation in the hippocampus. *Neuroscience* 304:109–121. <https://doi.org/10.1016/j.neuroscience.2015.07.021>
- Terlau H, Seifert W (1989) Influence of epidermal growth factor on long-term potentiation in the hippocampal slice. *Brain Res* 484(1–2):352–356
- Namba H, Zheng Y, Abe Y, Nawa H (2009) Epidermal growth factor administered in the periphery influences excitatory synaptic inputs onto midbrain dopaminergic neurons in postnatal mice. *Neuroscience* 158(4):1731–1741. <https://doi.org/10.1016/j.neuroscience.2008.10.057>
- Abe K, Saito H (1992) Epidermal growth factor selectively enhances NMDA receptor-mediated increase of intracellular Ca²⁺ concentration in rat hippocampal neurons. *Brain Res* 587(1):102–108
- Tohmi M, Tsuda N, Mizuno M, Takei N, Frankland PW, Nawa H (2005) Distinct influences of neonatal epidermal growth factor challenge on adult neurobehavioral traits in four mouse strains. *Behav Genet* 35(5):615–629. <https://doi.org/10.1007/s10519-005-5357-7>
- Futamura T, Kakita A, Tohmi M, Sotoyama H, Takahashi H, Nawa H (2003) Neonatal perturbation of neurotrophic signaling results in abnormal sensorimotor gating and social interaction in adults: implication for epidermal growth factor in cognitive development. *Mol Psychiatry* 8(1):19–29. <https://doi.org/10.1038/sj.mp.4001138>
- Nagano T, Namba H, Abe Y, Aoki H, Takei N, Nawa H (2007) In vivo administration of epidermal growth factor and its homologue attenuates developmental maturation of functional excitatory synapses in cortical GABAergic neurons. *Eur J Neurosci* 25(2):380–390. <https://doi.org/10.1111/j.1460-9568.2007.05297.x>
- Namba H, Nagano T, Jodo E, Eifuku S, Horie M, Takebayashi H, Iwakura Y, Sotoyama H et al (2017) Epidermal growth factor signals attenuate phenotypic and functional development of neocortical GABA neurons. *J Neurochem* 142:886–900. <https://doi.org/10.1111/jnc.14097>
- Sotoyama H, Namba H, Chiken S, Nambu A, Nawa H (2013) Exposure to the cytokine EGF leads to abnormal hyperactivity of pallidal GABA neurons: implications for schizophrenia and its modeling. *J Neurochem* 126(4):518–528. <https://doi.org/10.1111/jnc.12223>
- Ratray I, Smith E, Gale R, Matsumoto K, Bates GP, Modo M (2013) Correlations of behavioral deficits with brain pathology assessed through longitudinal MRI and histopathology in the R6/2 mouse model of HD. *PLoS One* 8(4):e60012. <https://doi.org/10.1371/journal.pone.0060012>
- Thomas R, Morris AWJ, Tai LM (2017) Epidermal growth factor prevents APOE4-induced cognitive and cerebrovascular deficits in female mice. *Heliyon* 3(6):e00319. <https://doi.org/10.1016/j.heliyon.2017.e00319>
- Thomas R, Zuchowska P, Morris AW, Marottoli FM, Sunny S, Deaton R, Gann PH, Tai LM (2016) Epidermal growth factor prevents APOE4 and amyloid-beta-induced cognitive and cerebrovascular deficits in female mice. *Acta Neuropathol Commun* 4(1):111. <https://doi.org/10.1186/s40478-016-0387-3>
- Gatto RG, Chu Y, Ye AQ, Price SD, Tavassoli E, Buenaventura A, Brady ST, Magin RL et al (2015) Analysis of YFP(J16)-R6/2 reporter mice and postmortem brains reveals early pathology and increased vulnerability of callosal axons in Huntington's disease. *Hum Mol Genet* 24(18):5285–5298. <https://doi.org/10.1093/hmg/ddv248>

25. Marottoli FM, Katsumata Y, Koster KP, Thomas R, Fardo DW, Tai LM (2017) Peripheral inflammation, apolipoprotein E4, and amyloid-beta interact to induce cognitive and cerebrovascular dysfunction. *ASN Neuro* 9 (4):1759091417719201. doi:<https://doi.org/10.1177/1759091417719201>
26. Cass DK, Flores-Barrera E, Thomases DR, Vital WF, Caballero A, Tseng KY (2014) CB1 cannabinoid receptor stimulation during adolescence impairs the maturation of GABA function in the adult rat prefrontal cortex. *Mol Psychiatry* 19(5):536–543. <https://doi.org/10.1038/mp.2014.14>
27. Flores-Barrera E, Thomases DR, Cass DK, Bhandari A, Schwarcz R, Bruno JP, Tseng KY (2017) Preferential disruption of prefrontal GABAergic function by nanomolar concentrations of the alpha7nACh negative modulator kynurenic acid. *J Neurosci* 37(33):7921–7929. <https://doi.org/10.1523/JNEUROSCI.0932-17.2017>
28. Menalled L, El-Khodori BF, Patry M, Suarez-Farinas M, Orenstein SJ, Zahasky B, Leahy C, Wheeler V et al (2009) Systematic behavioral evaluation of Huntington's disease transgenic and knock-in mouse models. *Neurobiol Dis* 35(3):319–336. <https://doi.org/10.1016/j.nbd.2009.05.007>
29. Berlanga-Acosta J, Gavalondo-Cowley J, Lopez-Saura P, Gonzalez-Lopez T, Castro-Santana MD, Lopez-Mola E, Guillen-Nieto G, Herrera-Martinez L (2009) Epidermal growth factor in clinical practice—a review of its biological actions, clinical indications and safety implications. *Int Wound J* 6(5):331–346. <https://doi.org/10.1111/j.1742-481X.2009.00622.x>
30. Gu X, Li C, Wei W, Lo V, Gong S, Li SH, Iwasato T, Itohara S et al (2005) Pathological cell-cell interactions elicited by a neuropathogenic form of mutant huntingtin contribute to cortical pathogenesis in HD mice. *Neuron* 46(3):433–444. <https://doi.org/10.1016/j.neuron.2005.03.025>
31. Dougherty SE, Hollimon JJ, McMeekin LJ, Bohannon AS, West AB, Lesort M, Hablitz JJ, Cowell RM (2014) Hyperactivity and cortical disinhibition in mice with restricted expression of mutant huntingtin to parvalbumin-positive cells. *Neurobiol Dis* 62:160–171. <https://doi.org/10.1016/j.nbd.2013.10.002>
32. Spanpanato J, Gu X, Yang XW, Mody I (2008) Progressive synaptic pathology of motor cortical neurons in a BAC transgenic mouse model of Huntington's disease. *Neuroscience* 157(3):606–620. <https://doi.org/10.1016/j.neuroscience.2008.09.020>
33. Skotte NH, Andersen JV, Santos A, Aldana BI, Willert CW, Norremolle A, Waagepetersen HS, Nielsen ML (2018) Integrative characterization of the R6/2 mouse model of Huntington's disease reveals dysfunctional astrocyte metabolism. *Cell Rep* 23(7):2211–2224. <https://doi.org/10.1016/j.celrep.2018.04.052>
34. Qi J, Kim M, Sanchez R, Ziaee SM, Kohtz JD, Koh S (2018) Enhanced susceptibility to stress and seizures in GAD65 deficient mice. *PLoS One* 13(1):e0191794. <https://doi.org/10.1371/journal.pone.0191794>
35. Gourfinkel-An I, Parain K, Hartmann A, Mangiarini L, Brice A, Bates G, Hirsch EC (2003) Changes in GAD67 mRNA expression evidenced by in situ hybridization in the brain of R6/2 transgenic mice. *J Neurochem* 86(6):1369–1378
36. Walker AG, Miller BR, Fritsch JN, Barton SJ, Rebec GV (2008) Altered information processing in the prefrontal cortex of Huntington's disease mouse models. *J Neurosci* 28(36):8973–8982. <https://doi.org/10.1523/JNEUROSCI.2804-08.2008>
37. Bristow LJ, Hutson PH, Thom L, Tricklebank MD (1993) The glycine/NMDA receptor antagonist, R-(+)-HA-966, blocks activation of the mesolimbic dopaminergic system induced by phencyclidine and dizocilpine (MK-801) in rodents. *Br J Pharmacol* 108(4):1156–1163
38. Takahata R, Moghaddam B (2003) Activation of glutamate neurotransmission in the prefrontal cortex sustains the motoric and dopaminergic effects of phencyclidine. *Neuropsychopharmacology* 28(6):1117–1124. <https://doi.org/10.1038/sj.npp.1300127>
39. Sokolowski JD, Salamone JD (1994) Effects of dopamine depletions in the medial prefrontal cortex on DRL performance and motor activity in the rat. *Brain Res* 642(1–2):20–28
40. Jinks AL, McGregor IS (1997) Modulation of anxiety-related behaviours following lesions of the prelimbic or infralimbic cortex in the rat. *Brain Res* 772(1–2):181–190
41. Jentsch JD, Tran A, Taylor JR, Roth RH (1998) Prefrontal cortical involvement in phencyclidine-induced activation of the mesolimbic dopamine system: behavioral and neurochemical evidence. *Psychopharmacology* 138(1):89–95
42. Drouin-Ouellet J, Sawiak SJ, Cisbani G, Lagace M, Kuan WL, Saint-Pierre M, Dury RJ, Alata W et al (2015) Cerebrovascular and blood-brain barrier impairments in Huntington's disease: potential implications for its pathophysiology. *Ann Neurol* 78(2):160–177. <https://doi.org/10.1002/ana.24406>
43. Lim RG, Quan C, Reyes-Ortiz AM, Lutz SE, Kedaigle AJ, Gipson TA, Wu J, Vatine GD et al (2017) Huntington's disease iPSC-derived brain microvascular endothelial cells reveal WNT-mediated angiogenic and blood-brain barrier deficits. *Cell Rep* 19(7):1365–1377. <https://doi.org/10.1016/j.celrep.2017.04.021>
44. Hsu YT, Chang YG, Chern Y (2018) Insights into GABAergic system alteration in Huntington's disease. *Open Biol* 8(12):180165. <https://doi.org/10.1098/rsob.180165>
45. Philpott AL, Cummins TDR, Bailey NW, Churchyard A, Fitzgerald PB, Georgiou-Karistianis N (2016) Cortical inhibitory deficits in premanifest and early Huntington's disease. *Behav Brain Res* 296:311–317. <https://doi.org/10.1016/j.bbr.2015.09.030>
46. Cummings DM, Andre VM, Uzgil BO, Gee SM, Fisher YE, Cepeda C, Levine MS (2009) Alterations in cortical excitation and inhibition in genetic mouse models of Huntington's disease. *J Neurosci* 29(33):10371–10386. <https://doi.org/10.1523/JNEUROSCI.1592-09.2009>
47. Spokes EG, Garrett NJ, Rossor MN, Iversen LL (1980) Distribution of GABA in post-mortem brain tissue from control, psychotic and Huntington's chorea subjects. *J Neurol Sci* 48(3):303–313
48. Perry TL, Hansen S, Kloster M (1973) Huntington's chorea. Deficiency of gamma-aminobutyric acid in brain. *N Engl J Med* 288(7):337–342. <https://doi.org/10.1056/NEJM197302152880703>
49. Reynolds GP, Pearson SJ (1990) Brain GABA levels in asymptomatic Huntington's disease. *N Engl J Med* 323(10):682–683. <https://doi.org/10.1056/NEJM199009063231014>
50. Reynolds GP, Pearson SJ (1987) Decreased glutamic acid and increased 5-hydroxytryptamine in Huntington's disease brain. *Neurosci Lett* 78(2):233–238
51. Iwakura Y, Nawa H (2013) ErbB1–4-dependent EGF/neuregulin signals and their cross talk in the central nervous system: pathological implications in schizophrenia and Parkinson's disease. *Front Cell Neurosci* 7:4. <https://doi.org/10.3389/fncel.2013.00004>
52. Sanchez-Huertas C, Rico B (2011) CREB-dependent regulation of GAD65 transcription by BDNF/TrkB in cortical interneurons. *Cereb Cortex* 21(4):777–788. <https://doi.org/10.1093/cercor/bhq150>
53. Chou CC, Modi JP, Wang CY, Hsu PC, Lee YH, Huang KF, Wang AH, Nan C et al (2017) Activation of brain L-glutamate decarboxylase 65 isoform (GAD65) by phosphorylation at threonine 95 (T95). *Mol Neurobiol* 54(2):866–873. <https://doi.org/10.1007/s12035-015-9633-0>
54. Rush DB, Leon RT, McCollum MH, Treu RW, Wei J (2012) Palmitoylation and trafficking of GAD65 are impaired in a cellular model of Huntington's disease. *Biochem J* 442(1):39–48. <https://doi.org/10.1042/BJ20110679>
55. Morfini GA, You YM, Pollema SL, Kaminska A, Liu K, Yoshioka K, Bjorkblom B, Coffey ET et al (2009) Pathogenic huntingtin

- inhibits fast axonal transport by activating JNK3 and phosphorylating kinesin. *Nat Neurosci* 12(7):864–871. <https://doi.org/10.1038/nn.2346>
56. Song M, Messing RO (2005) Protein kinase C regulation of GABAA receptors. *Cell Mol Life Sci* 62(2):119–127. <https://doi.org/10.1007/s00018-004-4339-x>
57. Bell-Horner CL, Dohi A, Nguyen Q, Dillon GH, Singh M (2006) ERK/MAPK pathway regulates GABAA receptors. *J Neurobiol* 66(13):1467–1474. <https://doi.org/10.1002/neu.20327>
58. Lund IV, Hu Y, Raol YH, Benham RS, Faris R, Russek SJ, Brooks-Kayal AR (2008) BDNF selectively regulates GABAA receptor transcription by activation of the JAK/STAT pathway. *Sci Signal* 1(41):ra9. <https://doi.org/10.1126/scisignal.1162396>
59. Li SH, Yu ZX, Li CL, Nguyen HP, Zhou YX, Deng C, Li XJ (2003) Lack of huntingtin-associated protein-1 causes neuronal death resembling hypothalamic degeneration in Huntington's disease. *J Neurosci* 23(17):6956–6964
60. Giampa C, Montagna E, Dato C, Melone MA, Bernardi G, Fusco FR (2013) Systemic delivery of recombinant brain derived neurotrophic factor (BDNF) in the R6/2 mouse model of Huntington's disease. *PLoS One* 8(5):e64037. <https://doi.org/10.1371/journal.pone.0064037>

Publisher's Note Springer Nature remains neutral with regard to jurisdictional claims in published maps and institutional affiliations.